PB81-154122

Semiconductor Technology Program
Progress Briefs

(U.S.) National Bureau of Standards
Washington, DC

Prepared for

Defense Advanced Research Projects Agency
Arlington, VA

Dec 79

PB81-154122

NBSIR 79-1591-5

Semiconductor Technology Program Progress Briefs

W. Murray Bullis, Editor

Electron Devices Division
Center for Electronics and Electrical
Engineering
National Engineering Laboratory
National Bureau of Standards
Washington, DC 20234

December 1979

Prepared for
The Defense Advanced Research Projects Agency
The National Bureau of Standards
The Division of Electric Energy Systems, Department of Energy
The Divison of Distributed Solar Technology, Department of Energy
The Defense Nuclear Agency
The Charles Stark Draper Laboratory
The Army Electronics Research and Development Command
The Air Force Avionics Laboratory
The Naval Material Command
The Naval Weapons Support Center
The Solar Energy Research Institute
The Naval Avionics Center
The Lewis Research Center, National Aeronautics & Space Administration
The Office of Naval Research

16

SEMICONDUCTOR TECHNOLOGY PROGRAM

TABLE OF CONTENTS

ABSTRACT — This report provides information on the current status of NBS work on measurement technology for semiconductor materials, process control, and devices. Results of both in-house and contract research are covered. Highlighted activities include: modeling of diffusion processes, analysis of model spreading resistance data, and studies of resonance ionization spectroscopy, resistivity-dopant density relationships in *p*-type silicon, deep level measurements, photoresist sensitometry, random fault measurements, power MOSFET thermal characteristics, power transistor switching characteristics, and gross leak testing. In addition, brief descriptions of new and selected on-going projects are given. The report is not meant to be exhaustive; contacts for obtaining further information are listed. Compilations of recent publications and publications in press are also included.

KEY WORDS — Electronics; integrated circuits; measurement technology; microelectronics; semiconductor devices; semiconductor materials; semiconductor process control; silicon.

Preface

This report covers results of work during the forty-fifth quarter of the NBS Semiconductor Technology Program. This Program serves to focus NBS research on improved measurement technology for the use of the semiconductor device community in specifying materials, equipment, and devices in national and international commerce, and in monitoring and controlling device fabrication and assembly. This research leads to carefully evaluated, well-documented test procedures and associated technology which, when applied by the industry, are expected to contribute to higher yields, lower cost, and higher reliability of semiconductor devices and to provide a basis for controlled improvements in fabrication processes and device performance. By providing a common basis for the purchase specifications of government agencies, improved measurement technology also leads to greater economy in government procurement. Financial support of the Program is provided by a variety of Federal agencies. The sponsor of each technical project is identified at the end of each entry in accordance with the following code: 1. The Defense Advanced Research Projects Agency; 2. The National Bureau of Standards; 3. The Division of Electric Energy Systems, Department of Energy; 4. The Division of Distributed Solar Technology, Department of Energy; 5. The Defense Nuclear Agency; 6. The C. S. Draper Laboratory; 7. The Army Electronics R&D Command; 8. The Air Force Avionics Laboratory; 9. The Naval Material Command; 10. The Naval Weapons Support Center; 11. The Solar Energy Research Institute; 12. The Naval Avionics Center; 13. The Lewis Research Center, National Aeronautics and Space Administration; and 14. The Office of Naval Research.

This report is provided to disseminate results rapidly to the semiconductor community. It is not meant to be complete; in particular, references to prior work either at NBS or elsewhere are omitted. The Program is a continuing one; the results and conclusions reported here are subject to modification and refinement. Further information may be obtained by referring to more formal technical publications or directly from responsible staff members, telephone: (301) 921-listed extension. General information, past issues of progress briefs, and a list of publications may be obtained from the Electron Devices Division, National Bureau of Standards, Washington, D.C. 20234, telephone: (301) 921-3786.

Semiconductor Technology Program

Progress Briefs

Modeling of Diffusion Processes

Fick's Law treats the diffusion coefficient as the factor of proportionality between the flux and the spatial gradient of a diffusing species. A recently reported model for impurity diffusion in semiconductors computes the flux in a different way by taking the spatial gradient of the product of the diffusion coefficient and the density of diffusing species. It was suggested that this modified form of Fick's Law implicitly accounts for electric-field effect. The significance of the difference between the two forms of the diffusion equation was explored by viewing diffusion as a Markov process, that is, as a stochastic process in which the diffusing species is undergoing a random walk wherein each step is independent of all other steps.

It was concluded from this analysis that the additional term in the modified form of Fick's Law, which contains the gradient of the diffusion coefficient, is a force term which may or may not be appropriate in the total flux equation. For the case of singly charged vacancy diffusion, and only for this case, there is a mathematical equivalence between this term and the force term associated with the self electric field. However, there is no physical relationship between this additional term and terms resulting from the effects of self or applied electric fields. It was therefore concluded that the conventional form of Fick's Law should be used to express the diffusion component of flux to which any force-driven components should be added explicitly to give the total flux. [Sponsor: 2] (J. R. Lowney, x3625)

Model Spreading Resistance Data

For uniform or shallow (<5 µm) diffused layers, the spreading resistance depends linearly on the logarithm of the probe spacing with a slope which is proportional to the sheet resistance of the layer and an intercept which is equal to the effective radius of the probes. Previous study of the relationship between the spreading resistance and probe spacing showed that for deeper diffusions the intercept cannot be interpreted in terms of the probe radius but that the slope is approximately proportional to the sheet resistance. To extend the study to ion-implanted layers, model spreading resistance data were generated from Gaussian resistivity profiles corresponding to implants at several beam energies and fluences into substrates with resistivity of 100 or 10^8 Ω·cm. The lower value was used to simulate the case of implantation into a substrate of the same conductivity type, while the higher was used to simulate the isolation which arises from the junction formed by implantation into substrates of opposite conductivity type.

In each case, data were generated for several probe spacings; the same effective electrical probe radius was used in all cases. At various points along the profile from the surface to the substrate, curves of spreading resistance as a function of the logarithm of the probe spacing were analyzed by linear regression to ascertain whether the slope was proportional to the incremental sheet resistance calculated directly from the model resistivity profile and whether the intercept was related to the probe radius used in the simulation. For the 10^8-Ω·cm substrate simulations, good agreement was obtained between the sheet resistance calculated from the slope and that calculated from the resistivity profile. For the 100-Ω·cm substrate simulations, fluences of the order of 10^{13} cm^{-2} were required to achieve comparable agreement. For both cases, the agreement between the intercepts and the probe radius used in the simulations was generally not satisfactory which suggests that the probe-spacing experiment is not an accurate method for determining the probe radius. However, the results of these simulations and those previously reported for deep diffusions suggest that probe-spacing experiments may be effectively used to determine the sheet resistance of small geometry specimens which contain diffusions or implants into substrates of the opposite conductivity or, if the substrate resistivity is high enough, into substrates of the same conductivity type. This result is especially important where specimen size precludes accurate sheet resistance measurement by the four-probe method but where measurements of this quantity are important for process control and process modeling. [Sponsor: 1]

(J. H. Albers, x3625)

Resonance Ionization Spectroscopy

A single atom of sodium was detected by resonance ionization spectroscopy (RIS) in a proportional counter filled with sodium-contaminated P-10 (90% argon plus 10% methane) gas to a pressure of 94 Torr. The apparatus used for this experiment is shown schematically in the accompanying figure. A laser of wavelength λ_1 = 588.995 nm induces the 3s-3p transition (ground state to one of

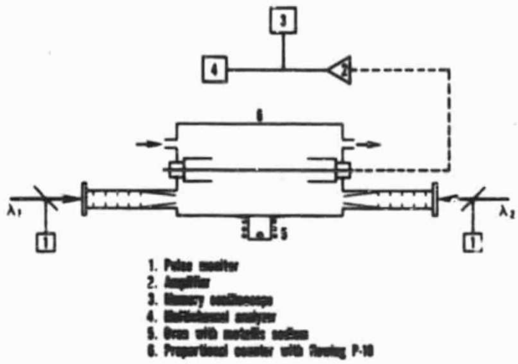

Schematic diagram of apparatus for resonance ionization spectroscopy experiment.

the "D" levels), and a second laser with wavelength λ_2 = 568.820 nm induces the 3p-4d transition leading to a level only 0.855 eV below the ionization potential in sodium. From this highly excited level, either laser λ_1 (2.104 eV) or λ_2 (2.179 eV) can induce photoionization, releasing an atomic electron with very low kinetic energy. This photoelectron is accelerated by the electric field in the counter, drifting towards the anode to develop a Townsend avalanche in the gas.

The pulsed dye lasers are pumped by a coaxial xenon flashlamp and tuned to the appropriate wavelength by a dispersive system in the laser cavity. The radiation is collimated to a beam 3 mm in diameter by a reducing telescope provided with a spatial filter. The intersection of the two beams in the counter generates an active volume of about 100 mm^3. The pulse energy was typically 0.5 J; the asymmetric triangular pulse has a rise time of about 100 ns and a base width of about 700 ns. The counter was calibrated for single-electron detection with uv light from a small mercury lamp appropriately collimated to illuminate a small area of the counter cathode. The normalized pulse-height distribution was found to fit the expected probability distribution for a series of single-electron events. Calibration for several primary electrons (up to 350) was done by use of x-ray fluorescence lines from a variety of metals. The average number of primary electrons generated by each line, which is proportional to the line energy, was a linear function of the peak amplitude of the signal.

In the single-atom detection experiment, a controlled amount of sodium vapor was injected into the counter from the small oven attached to it. The sodium-RIS signal appeared only when both lasers were tuned to the proper wavelengths; it disappeared when either laser was detuned or blocked. Single-atom detection was confirmed by decreasing the amount of injected sodium until the RIS signal disappeared; at sodium levels just above extinction, the signal amplitude distribution was consistent with the single-electron pulse height distribution. [Sponsors: 2, 14]

(S. Mayo, x3625, and T. B. Lucatorto,* x2031)

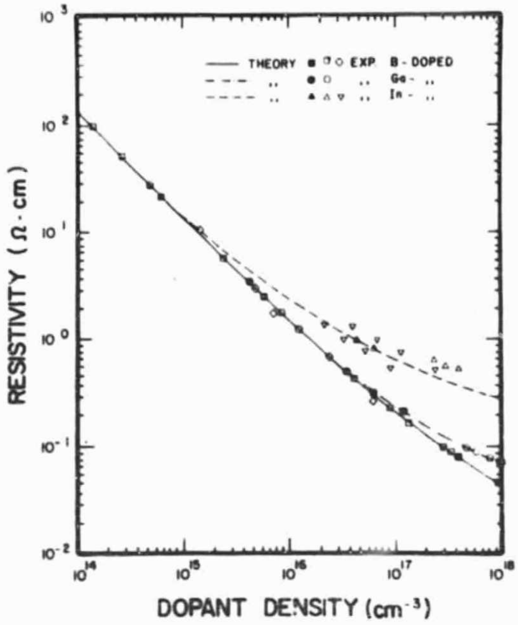

Resistivity as a function of dopant density for boron-, gallium-, and indium-doped silicon at 300 K. Theoretical curves are shown as lines, experimental data obtained in the present work are shown as solid symbols, and data obtained from the literature are shown as open symbols.

Resistivity-Dopant Density Evaluation

Theoretical expressions were derived at the University of Florida to compute hole mobility and resistivity as functions of dopant density and temperature for silicon doped with boron, gallium, or indium. The valence band of silicon was represented by a three-band model which takes into account the nonparabolic nature of the bands. This attribute of the valence band is included in the effective mass calculations. Contributions from scattering by acoustical and optical phonons, ionized impurities, and neutral impurities were considered in the calculation of average relaxation time. In addition, the model also takes into account the effect of hole-hole scattering on both lattice and ionized impurity scattering relaxation times and the effect of interband transitions on the acoustic phonon scattering relaxation time. Resistivity and dopant density measurements were made as a function of temperature over the range from 100° to 400°C on silicon wafers doped with boron, gallium, or indium. Agreement between the experimental and theoretical results was within 10% over the entire temperature range. The accompanying figure shows the calculated resistivity-dopant density curves for a temperature of 300 K together with experimental data from this study and from

* NBS Radiation Physics Division.

the literature. The differences which arise because of differences in ionization energy are clearly evident. [Sponsor: 1] (W. R. Thurber,* x3625)

Deep Level Measurements

In making deep level measurements to identify impurities in a test specimen, one determines the activation energy and prefactor associated with carrier emission from one or more centers and relates these to values which have been established from measurements on intentionally contaminated specimens. Calculations were made to determine the deep level transient spectroscopy (DLTS) response which might be obtained from a specimen which contains two impurity centers relatively closely spaced in energy. The DLTS signals for several pairs of levels were calculated for a range of sampling times typical of those used in experiments. From these curves, each of which had a single maximum (although some appeared broader and somewhat distorted when compared with signals computed for single isolated levels), the apparent activation energies (ΔE) and prefactors (B) were determined and compared with the originally assumed parameters. The results of two representative cases are shown in the accompanying table. The parameters of the composite signal differ from those of either of the two assumed levels and thus would obscure the proper identification. Further work is underway to study experimental procedures for determining that interference of this type are present and ways of separating peaks associated with closely spaced levels. [Sponsor: 3] (R. Y. Koyama, x3625)

Parameters for Model DLTS Calculations

	Case 1	Case 2
ΔE_1, eV	0.2018	0.2036
B_1, $s^{-1}.K^{-2}$	3.115×10^6	2.48×10^6
ΔE_2, eV	0.175	0.187
B_2, $s^{-1}.K^{-2}$	3.115×10^6	2.48×10^6
ΔE, eV	0.212	0.2018
B, $s^{-1}.K^{-2}$	9.71×10^6	3.115×10^6

Note — In both cases, level 2 is assumed to be present with half the density of level 1.

Photoresist Sensitometry

Experimental work was completed which verifies the applicability of Van Kreveld's additivity law to exposures of positive photoresists and therefore also confirms the suitability of the techniques for determining exposure characteristics of photoresists which had been postulated some years ago. The law had been previously shown to apply when films of a commonly used positive resist were successively exposed to filtered radiation of 356, 405, and 436 nm. In these experiments, exposures were made both for equal times and for times adjusted to compensate for variations in the transmittance of the narrow-pass filters so that the exposures matched the relative irradiance of a mercury arc lamp at each of the three wavelengths. When these experiments were repeated with exposure first to the 436-nm irradiation followed successively by exposure to the 405- and 365-nm irradiation, the experimental exposure *vs.* exposed depth curve also agreed well with calculations based on Van Kreveld's Law.

Another set of experiments was carried out in which resist films were exposed simultaneously to filtered radiation of wavelengths of 365, 405, and 436 nm from the mercury arc lamp. A specially designed jig was used for these experiments. Three mirrors were mounted in the plane bisecting and normal to the mercury arc lamp at azimuthal angles of 120° from each other. These mirrors, in

* NBS Contact

turn, refl-cted light vertically upward through respective lenses and narrow band filters onto a resist-coated glass plate approximately 76 cm above the lamp and on the same center line. This created a superposition of impinging light of three wavelengths about 4° from the normal on the resist-coated plate. The actual measured intensities used for the respective exposures were within 5% of those calculated from Van Kreveld's additivity law and monochromatic exposure data except for the smallest exposures where differences of up to 20% were found. For these small exposures, the experimental errors are greatest.

Measurements of the power density spectrum of the mercury arc lamp confirmed the hypothesis that unaccounted-for background radiation (radiation from the continuum existing between the principal mercury arc lines) was responsible for the previously reported discrepancy between the measured and calculated exposure data when the resist was exposed by unfiltered radiation from the lamp. It was found that (1) the principal lines at 365, 405, and 436 nm were only 3 to 4 nm wide (FWHM), one-third or less than the published spectral width, and (2) the energy radiated at wavelengths between the principal lines was 35% of the energy contained in these lines. [Sponsor: 1] (D. B. Novotny, x3621)

Random Fault Measurements - I

Test results from a random access fault structure can be used to detect, identify, and analyze a variety of fault mechanisms introduced during the fabrication of integrated circuits. The structure allows one to determine the relative density of different faults which limit process yield without previous knowledge of what fault types might be expected. In some cases, it detects faults which cannot be detected by single-fault-type random fault test structures. A prototype structure which consists of a 10 by 10 array of electrically isolated *n*- or *p*-channel MOSFETs has been implemented on test pattern NBS-16. This test pattern is being used to develop methods to assess the electrical performance and yield potential of radiation-hardened, silicon-gate CMOS/SOS LSI circuits. The structures are repeated at intervals across a wafer so that the threshold voltage (V_T) at a drain current of 1 µA with gate tied to drain, source-drain breakdown voltage (V_B) at a drain current of 10 µA with gate tied to source, and source-to-drain leakage current (I_C) at a drain voltage of 10 V with gate tied to source can be measured on a statistically significant number of individual MOSFETs. These results are then compared with failure criteria which define the parametric limits required for satisfactory circuit operation. In addition, open and short circuits in the structure can be detected.

Typical results from a wafer representative of a lot with relatively low device yield are shown in the accompanying

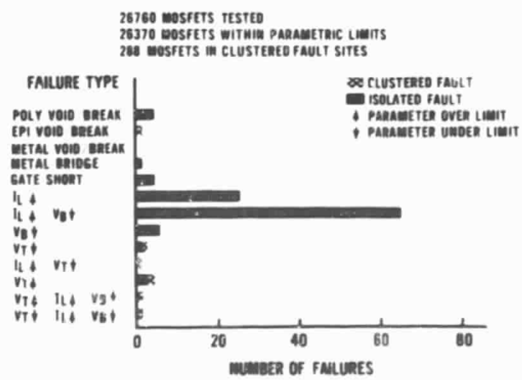

Test results from random access fault structures on a wafer representative of a lot with relatively low device yield.

figure. Failure of two or more adjacent devices to meet a given criterion is treated as a single clustered fault. In this example, 40 of the MOSFETs could not be tested because of opens or shorts in the common connections between the MOSFET and the probe pad. The measured parameters of 26370 of the 26760 tested MOSFETs fell within the defined limits; there were 102 isolated faults, and 288 MOSFETs were contained in the clustered-fault sites. From these results, it can be seen that the dominant failure type is an excess source-to-drain leakage current, usually coupled with low breakdown voltage. Analysis of test results suggests that this failure mode, which had not been anticipated at the time the test pattern was designed, was the primary contributor to yield degradation of the accompanying product wafer lot. This failure mode would not have been detected from test results of other test structures on the pattern. [Sponsor: 8] (L. W. Linholm, x3541)

Random Fault Measurements - II

One of the two random fault test structures on test pattern NBS-16 is designed to measure gate and field oxide integrity in a CMOS-SOS process. A composite drawing of this structure is shown in the accompanying figure. The structure is comprised of five layers on a sapphire substrate: n^- epitaxial silicon lines, 80-nm thick gate oxide, p^+ polysilicon lines running at right angles to the epi lines, 600-nm thick field oxide, and aluminum metallization. At the crossovers, the poly and epi lines are separated by gate oxide. The poly lines are grouped to form seven arrays with 57, 114, 225, 375, 750, 1500, and 3000 crossovers. Each array is covered with the metallization layer which is separated from the poly or epi lines by field oxide. The polysilicon and metallization in each array are each connected to a probe pad; all of the epi lines in each group of arrays are connected to a single probe pad. There are 95 such groups of seven arrays on a wafer fabricated with test pattern NBS-16. Preliminary analysis of initial measurements of leakage current between pairs of conducting layers on wafers taken from three processed lots suggests that the array sizes are appropriate for evaluating the process under study. However, in some cases, the origin of the leakage current cannot be established unambiguously; work is underway to determine the causes of the various

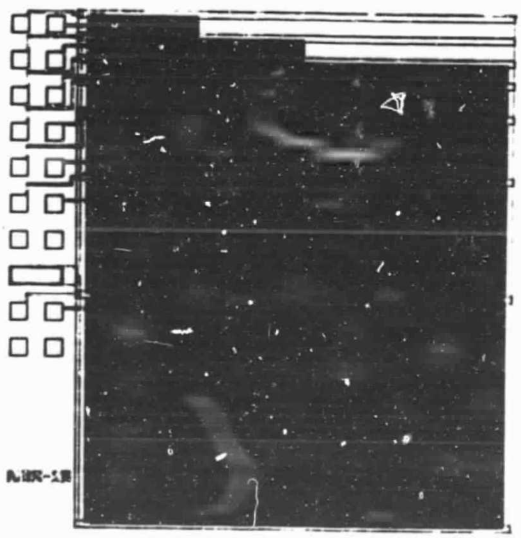

Composite drawing of random fault test structure for evaluating gate and field oxide integrity in a CMOS-SOS process. The n^- epi lines which run vertically are connected together by the wide horizontal bars and brought out to the double probe pad E. The poly lines run horizontally; each array is connected to a separate probe pad P. Each array is completely covered by metallization connected to a separate probe pad M.

ambiguities, to investigate methods of analysis by which the ambiguities might be removed, and to evaluate design modifications to provide better separation of leakage current sources. [Sponsors: 1,8] (M. A. Mitchell and L. W. Linholm, x3541)

Power MOSFET Characterization

Three techniques for measuring the temperature of silicon power MOS field-effect transistors (MOSFETs) are being investigated. Two of the techniques employ temperature-sensitive electrical parameters (TSPs) of the device, the forward voltage of the drain-body diode (V_{DB}) at constant low current, and the applied gate voltage (V_G) at constant drain current. The third is a direct measurement of the surface temperature using an automated infrared microradiometer (IRM).

The temperature variation of V_{DB} is both linear and well characterized. Measurement of MOSFET temperature with this TSP is similar to a method used to measure the temperature of bipolar transistors using the forward voltage of the collector-base diode as the TSP. However as in the bipolar case, the diode senses only an average chip temperature because it occupies a large area of the chip, whereas the heat source (defined by the channel region) occupies a very small area. Also, the large electrical capacitance of the forward-biased diode makes the required electrical switching extremely slow.

Much less is known about the temperature dependence of V_G. It is known that this voltage can increase, decrease, or remain constant with temperature depending upon the value of the applied gate voltage and the channel characteristics. Preliminary results suggest that V_G varies linearly with temperature, at least for drain currents up to about 3 A; the temperature coefficient varies from about -6 mV/°C at 10 mA to about -4 mV/°C at 1 A to about -2 mV/°C at 3 A. At higher drain currents, typical of those encountered in device operation, the temperature coefficient would be expected to approach or pass through zero; therefore, to obtain adequate sensitivity, it may be desirable to use a switching method, similar in concept to the standard method employed for measuring the junction temperature of bipolar transistors with the emitter-base voltage (V_{EB}) as the TSP. In this method, the device is operated at the conditions for which the temperature is desired and then rapidly switched to a low value of drain current for measurement of the V_G.

If the temperature measured by the IRM is to be accurate, the power MOSFET surface must be coated with a uniform, high emissivity film because the very fine metallization patterns on these devices cause the spatial variation of surface emissivity to be extremely rapid and large. In the present work, a flat-black, commercial spray paint with low carbon content (to reduce electrical conductivity) is used.

Preliminary comparative measurements of the temperatures determined by the three methods confirm that the temperature indicated with V_{DB} as the TSP is very nearly equal to the average chip temperature as determined by an unweighted spatial averaging of the IRM results. However, contrary to results found with the use of V_{EB} in bipolar devices, use of V_G as the TSP results in a device temperature in excess of the peak temperature as determined by the IRM. This may occur because the spatial resolution of the IRM is not sufficient to resolve the peak gate temperature or because of errors in the gate voltage measurement method. These possibilities are being investigated further. [Sponsor: 2] (D. L. Blackburn, x3621)

Transistor Switching Characteristics

Work was undertaken to develop improved methods for characterizing the switching properties, particularly the reverse-bias safe operating limits, of power transistors. Initially, the effect of the magnitude of the base current, I_{BR}, on transistor switching characteristics is being studied. Previous work had shown that the magnitude of I_{BR} has a strong influence on the reverse-bias safe operating limits of silicon n^+-p-ν-n^+ power transistors. Generally, as I_{BR} is increased, the voltage at which second breakdown occurs decreases. It was also observed that for the turnoff of these devices, a time interval exists which occurs during, but is distinct from, the traditional storage time. During this newly observed interval, designated the dynamic saturation time, the collector voltage slowly rises as the collector current remains nearly constant. It was found that as much as 30% of the total energy dissipated during turnoff may occur during this interval. It is therefore important to understand its cause and effects.

Observation of the time variation of the base-emitter voltage during turnoff shows that current focusing to the center of the emitter fingers does not begin to occur until after the device has entered dynamic saturation. This is consistent with the idea that the effective base width (i.e., the metallurgical base width plus the width of the conductivity-modulated portion of the lightly doped (ν) collector region) begins to decrease when the device enters dynamic saturation. Thus the slow rise

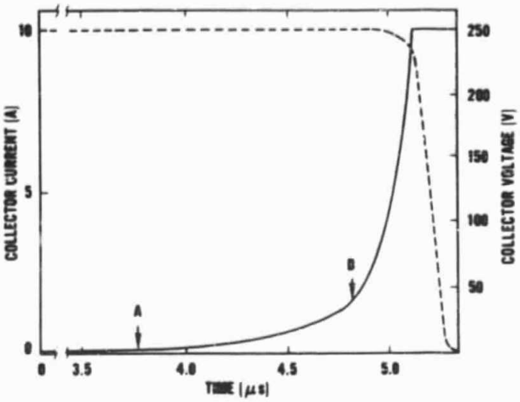

Current (dashed curve) and voltage (solid curve) transients of an n^+-p-ν-n^+ power transistor following switching of the base current from +4 A to -0.5 A at time zero. The transistor is operating in a dynamic saturation condition between the points labeled A and B on the voltage trace. In the dynamic saturation region, the collector voltage increases slowly and the collector current is essentially constant as discussed in the text.

of the collector voltage can be attributed to an increased resistive voltage drop as stored charge is being removed from the collector, narrowing the width of conductivity-modulated portion of the ν-region of the collector.

The finding that current focusing does not occur until the device enters dynamic saturation also provides an explanation of the dependence of the second-breakdown voltage on base current. For reverse-bias second breakdown to occur, a high current density is required; the high density is realized as a result of the current focusing. Thus, the magnitude of I_{BR} during dynamic saturation should affect the second breakdown characteristics, but the magnitude before dynamic saturation (i.e., during classical saturation) should have no effect. This was verified experimentally;

the voltage at which second breakdown occurred was observed to be exactly the same if the value of I_{BR} to which the device was switched after dynamic saturation began was applied instead during the entire turnoff time. Thus, turnoff time may be reduced with minimum risk of second breakdown if I_{BR} is large at the start of the turnoff cycle but is reduced to a small value near the end. [Sponsor: 13]

(D. L. Blackburn, x3621)

Gross Leak Testing

Although the correlation between gross leaks in hermetically packaged semiconductor devices and their failure rates is clear cut, the dry gas hermetic test methods currently in use are far from satisfactory. The commonly used helium mass spectrometer and radioisotope leak tests are based on back pressurization techniques. At present the limitation in applying these procedures to the gross leak range is the rapid depletion of the gas from the package interior which leads to inability to detect large leaks. A new noncontaminating, quantitative dry gas test method has been developed to eliminate these problems. This method is intended for use in the leak size range from about 10^{-5} to about 1 atm·cm^3/s. It employs a rapid gas cycling technique to extend the upper range of the helium mass spectrometer leak detector by reducing the delay between the pressurization phase and the detection of the tracer gas which has penetrated the package. In addition, the environmental conditions during the test are tailored so that a simple quantitative relationship based on viscous flow theory exists between the true and measured leak values.

Two modes of operation have been employed. One mode utilizes a single test chamber for both pressurization and detection, while the second mode separates these functions. Present test times for either mode are of the order of 8 s. In the single chamber mode, the process occurs in four rapid steps. The package is pressurized for about 2 s in an atmosphere of nitrogen which contains about 1% helium. The chamber is then vented to the atmosphere and the remaining excess gas exhausted within a fraction of a second. After the chamber is refilled with a neutral gas such as nitrogen or dry air to further dilute the helium concentration in the chamber, it is exhausted a second time and pumped to low enough pressure for the helium leak detector to be valved in. This process, which is carried out under automatic control, reduced the partial pressure of helium in the ambient around the test package by a factor of about 10^7 within a few seconds. The second mode of operation is inherently simpler and less subject to sorption effects, but it requires rapid transfer of the test specimen between the pressurizing and detection chambers; in this mode, the pressurization chamber is exhausted only once.

Measurements were made on a group of glass capsules fabricated with capillary leaks which were measured initially by means of an absolute procedure. Leak sizes determined from the experimentally measured leak rate appear to be within ±50% of the true (initial) value over the leak size range from 10^{-5} to 0.5 atm·cm^3/s. Closer agreement is expected after corrections are made for leak detector response time. [Sponsor: 2]

(S. Ruthberg, x3621)

Linewidth Seminar Rescheduled

The third in the series of measurement seminars on integrated circuit linewidth measurements has been rescheduled for July 15-18, 1980 at NBS/Gaithersburg. The primary emphasis in this seminar will be on the measurement of widths of features in the range 0.5 to 10 μm on silicon wafers. The seminar will consist of lectures, laboratory demonstrations, hands-on training with optical microscope systems, and small group discussions of industry measurement problems. [Sponsor: 2] (E. C. Cohen, x3786, and J. M. Jerke, x3621)

New Topic . . .

Carbon in Silicon — Average carbon densities typically present in silicon crystals grown by the Czochralski process range from 10^{16} to 10^{17} cm^{-3}. Although as a neutral substitutional impurity carbon has no direct effects on device performance, it has recently been implicated in a wide range of deleterious indirect effects such as the nucleation of intrinsic defects, oxide precipitation, the "X" centers in indium-doped silicon, gold diffusion, and dopant distribution. A new project to study carbon in silicon was initiated. The first step in this project is to develop methods for measuring the carbon distribution across production wafers. These methods will then be applied in a thorough study of the role of carbon in silicon, from its initial distribution to the effects of processing. [Sponsor: 2] (A. Baghdadi, x3625)

Work in Progress . . .

A procedure developed for adjusting an optical microscope to operate in Kohler illumination is being documented in the format of an ASTM Practice. This operating mode provides uniform illumination of the specimen, reduces stray light, and results in bright images with good contrast. The procedure includes definitions of appropriate terms and specifications for the necessary equipment; it describes techniques for setting up the microscope with either transmitted or reflected illumination. In addition, the procedure tells the user how to set the ratio of condenser numerical aperture to objective numerical aperture equal to two thirds in order to provide images with steep edge gradients. This procedure is an essential part of the instructions currently being developed for using the photomask-like chromium-on-glass artifacts (soon to be made available by NBS as standard reference material SRM 474) to calibrate an optical microscope for linewidth measurements in the 0.5- to 10-μm regime. These instructions will be applicable to most types of measurement systems, such as filar, image-shearing, and video-micrometer systems, used throughout the microelectronics industry to measure linewidths on photomasks. [Sponsor: 1] (J. M. Jerke, x3621)

The optical spectra of the deepest known sulfur center in silicon are being studied. Specimens were prepared by diffusing natural sulfur (95% ^{32}S) or isotopically enriched sulfur (90% ^{34}S) into *p*-type silicon doped with boron to a density of about 3×10^{16} cm^{-3}. The diffusions were carried out at 1350°C for about 200 h in an evacuated, sealed quartz tube. In contrast to earlier studies of this center by isothermal transient capacitance and thermally stimulated current measurements, no significant isotopic shift of the energy level was observed. It remains to be determined whether the difference occurs because the same center is not being observed in the two experiments or because the center responds differently to the two measurement techniques. [Sponsor: 2] (R. A. Forman, x3625)

Recent Publications . . .

*Johnson, N. M., Bartelink, D. J., Gold, R. B., and Gibbons, J. F., Constant-Capacitance DLTS Measurement of Defect-Density Profiles in Semiconductors, *J. Appl. Phys.* 50, 4828-4833 (July 1979).

Koyama, R. Y., and Buehler, M. G., Novel Variable-Temperature Controllable Chuck for Use in the Detection of Deep Levels in Processed Semiconductor Wafers, *Rev. Sci. Instrum.* 50, 983-987 (August 1979).

Leedy, T. F., Large Scale Integration Digital Testing — An Annotated Bibliography, 1969 to 1978, NBS Tech. Note 1102 (August 1979).

*Quate, C. F., Atalar, A., and Wickramasinghe, H. K., Acoustic Microscopy with Mechanical Scanning — A Review, *Proc. IEEE* 67, 1092-1114 (August 1979).

Sawyer, D. E., and Schafft, H. A., *Semiconductor Measurement Technology:* NBS/DOE Workshop, Stability of (Thin Film) Solar Cells and Materials, NBS Spec. Publ. 400-58 (August 1979).

*Schwarz, S. A., and Helms, C. R., A Statistical Model of Sputtering, *J. Appl. Phys.* 50, 5492-5499 (August 1979).

*Sulouff, R. E., Investigation of Moisture Measurement, Failure Rate, and Leak Rate and Study of Moisture Infusion, NBS-GCR-79-170 (August 1979).

Harman, G. G., *Semiconductor Measurement Technology:* Nondestructive Tests Used to Insure the Integrity of Semiconductor Devices, with Emphasis on Acoustic Emission Techniques, NBS Spec. Publ. 400-59 (September 1979).

Scace, R. I., Technology of Semiconductor Manufacturing, Product Development, and Product Types, Appendix to *A Report on the U.S. Semiconductor Industry*, U.S. Dept. of Commerce (September 1979).

Buehler, M. G., Comprehensive Test Patterns with Modular Test Structures: The 2 by N Probe-Pad Array Approach, *Solid State Technology* 22 (10), 89-94 (October 1979).

*Quate, C. F., The Acoustic Microscope, *Sci. Am.* 241 (4), 62-70 (October 1979).

Publications in Press . . .

Blackburn, D. L., *Semiconductor Measurement Technology:* An Automated Photovoltaic System for the Measurement of Resistivity Variations in High-Resistivity Circular Silicon Slices, NBS Spec. Publ. 400-52.

Blackburn, D. L., and Berning, D. W., Reverse-Bias Second Breakdown in Power Transistors, *Proc. Electrical Overstress/Electrostatic Discharge Symp.*, Denver, CO, September 25-27, 1979.

Bullis, W. M., Ed., Semiconductor Measurement Technology, Progress Report, October 1, 1976 to March 31, 1977, NBS Spec. Publ. 400-38.

Bullis, W. M., Metrology for Submicrometer Devices and Structures, *Proc. Microcircuit Engineering '79 — Microstructure Fabrication*, Aachen, West Germany, September 25-27, 1979.

Carver, G. P., Linholm, L. W., and Russell, T. J., The Use of Microelectronic Test Structures to Characterize IC Materials, Processes, and Processing Equipment, *Solid State Technology*.

Ehrstein, J. R., Spreading Resistance Calibration for Gallium- or Aluminum-Doped Silicon, *J. Electrochem. Soc.*

Ehrstein, J. R., Two-Probe (Spreading Resistance) Measurements for Evaluation of Semiconductor Materials and Devices, *Nondestructive Evaluation of Semiconductor Materials and Devices*, NATO Advanced Study Institute, Frascati, Italy, September 18-30, 1978.

Galloway, K. F., Mayo, S., and Roitman, P., Radiation Levels Associated with Advanced Lithographic Techniques, *J. Electrochem. Soc.*

*Grunthaner, F. J., Grunthaner, P. J., Vasquez, R. P., Lewis, B. F., Maser-

* Reports of Contract Research.

jian, J., and Madhukar, A., Local Atomic and Electronic Structure of Oxide/GaAs and SiO_2/Si Interfaces Using High-Resolution XPS, *J. Vac. Sci. Tech.*

*Ham, W. E., *Semiconductor Measurement Technology:* Comprehensive Test Pattern and Approach for Characterizing SOS Technology, NBS Spec. Publ. 400-56.

Harman, G. G., Nondestructive Tests Used to Insure the Integrity of Semiconductor Devices with Emphasis on Passive Acoustic Techniques, *Nondestructive Evaluation of Semiconductor Materials and Devices*, NATO Advanced Study Institute, Frascati, Italy, September 18-30, 1978.

Jerke, J. M., Ed., *Semiconductor Measurement Technology:* Accurate Linewidth Measurements on Integrated-Circuit Photomasks, NBS Spec. Publ. 400-43.

*Kasden, H. L., Linewidth Measurement by Diffraction Pattern Analysis, NBS-GCR-79-175.

Kenney, J. M., *Semiconductor Measurement Technology:* Modulation Measurements for Microwave Mixers, NBS Spec. Publ. 400-16.

Larrabee, R. D., and Thurber, W. R., Theory and Application of a Two-Layer Hall Technique, *IEEE Trans. Electron Devices*.

Li, S. S., *Semiconductor Measurement Technology:* The Theoretical and Experimental Study of the Temperature and Dopant Density Dependence of the Hole Mobility, Effective Mass, and Resistivity in Boron-Doped Silicon, NBS Spec. Publ. 400-47.

Linholm, L. W., Carver, G. P., and Russell, T. J., The Use of Microelectronic Test Structures to Characterize IC Materials, Processes, and Processing Equipment, *Proc. Measurement Sciences Conf.*, San Luis Obispo, CA, November 30-December 1, 1979.

Myers, D. R., and Phillips, W. E., Observation of Unequal Densities for Sulfur Defects in Silicon Predeposition by Low Fluence Ion Implantation, *J. Electron. Mat.*

Myers, D. R., Wilson, R. G., and Comas, J., Considerations of Ion Channeling for Semiconductor Microstructure Fabrication, *J. Vac. Sci. Tech.*

Nyyssonen, D., Spatial Coherence: The Key to Accurate Optical Micrometrology, *Proc. SPIE Seminar on Applications of Optical Coherence*, San Diego, CA, August 30, 1979.

Phillips, W. E., Improved Thermometry for Deep Level Measurements, *J. Phys. E.*

Phillips, W. E., Koyama, R. Y., and Buehler, M. G., Suppression of Measurement Interferences from Interface States and Mobile Ions in Thermally Stimulated Current Measurements in an MOS Capacitor, *J. Electrochem. Soc.*

Sawyer, D. E., Kessler, H. K., and Schafft, H. A., Measurement Techniques for Solar Cells, Quarterly Report for the Period April 1 to June 30, 1978, NBSIR 79-1909.

Sawyer, D. E., and Kessler, H. K., Laser Scanning of Solar Cells for the Display of Cell Operating Characteristics and Detection of Cell Defects, *IEEE Trans. Electron Devices*.

Thurber, W. R., A Comparison of Measurement Techniques for Determining Phosphorus Concentrations in Semiconductor Silicon, *J. Electron. Mat.*

*Wilson, R. G., and Comas, J., Atomic and Carrier Depth Distributions of Beryllium Implanted in Silicon and Their Thermal Redistribution, *J. Vac. Sci. Tech.*

*Wilson, R. G., and Weglein, R. D., Acoustic Material Signatures Using the Reflection Acoustic Microscope, *Proc. 1st Internat. Symp. Ultrasonics Matls. Characterization*, Washington, DC, June 8-10, 1978.

* Reports of Contract Research.

NBS-114A (REV. 9-78)

U.S. DEPT. OF COMM. BIBLIOGRAPHIC DATA SHEET	1. PUBLICATION OR REPORT NO. NBSIR 79-1591-5	[redacted]	[redacted]

4. TITLE AND SUBTITLE

Semiconductor Technology Program — Progress Briefs

5. Publication Date

December 1979

[redacted]

7. AUTHOR(S)

W. Murray Bullis, Editor

8. Performing Organ. Report No.

9. PERFORMING ORGANIZATION NAME AND ADDRESS

NATIONAL BUREAU OF STANDARDS
DEPARTMENT OF COMMERCE
WASHINGTON, DC 20234

[redacted]

11. Contract/Grant No.

See item 15.

12. SPONSORING ORGANIZATION NAME AND COMPLETE ADDRESS *(Street, City, State, ZIP)*

NBS, Washington, DC 20234; ARPA, Arlington, VA 22209; DNA, Washington, DC 20305; Dept. of Energy, Washington, DC 20545; C. S. Draper Laboratory, Cambridge, MA 02139; AFAL, Wright-Patterson AFB, OH 45433; Army Electronics R&D Command, Ft. Monmouth, NJ 07703; NavMat Command, Hdqtrs., Washington, DC 20360; NWSC, Crane, IN 47522; SERI, Golden, CO 80401; NASA-Lewis Research Center, Cleveland, OH 44135; ONR, Arlington, VA 22217.

13. Type of Report & Period Covered

Interim
July to September 1979

[redacted]

15. SUPPLEMENTARY NOTES

ARPA Order 2397, Program Code 9Y10; DNA IACRO 79-821; Dept. of Energy, Interagency Agreement EA-77-A01-6010, T. O. A021-EES and T. O. A054-SE; C. S. Draper Laboratory, P. O. DL-H-162208 (Navy contract N 00030-78-C-0100); AFAL, MIPR FY11757N2062; Army Electronics, R&D Command, P. O. 78-09423; NavMat Command, P. O. N0003778IP89010; NWSC, P. O. N0016479WR30015; SERI, EG-77-C-01-4042; NavAir, MIPR N0016379MP930006; NASA-Lewis, C-32818-D; ONR, N00014-79-F-0051.

16. ABSTRACT *(A 200-word or less factual summary of most significant information. If document includes a significant bibliography or literature survey, mention it here.)*

This report provides information on the current status of NBS work on measurement technology for semiconductor materials, process control, and devices. Results of both in-house and contract research are covered. Highlighted activities include: modeling of diffusion processes, analysis of model spreading resistance data, and studies of resonance ionization spectroscopy, resistivity-dopant density relationships in *p*-type silicon, deep level measurements, photoresist sensitometry, random fault measurements, power MOSFET thermal characteristics, power transistor switching characteristics, and gross leak testing. In addition, brief descriptions of new and selected on-going projects are given. The report is not meant to be exhaustive; contacts for obtaining further information are listed. Compilations of recent publications and publications in press are also included.

17. KEY WORDS *(six to twelve entries; alphabetical order; capitalize only the first letter of the first key word unless a proper name; separated by semicolons)*

Electronics; integrated circuits; measurement technology; microelectronics; semiconductor devices; semiconductor materials; semiconductor process control; silicon.

18. AVAILABILITY	19. SECURITY CLASS (THIS REPORT)	21. NO. OF PRINTED PAGES
[x] Unlimited	UNCLASSIFIED	16
[ ] For Official Distribution. Do Not Release to NTIS	20. SECURITY CLASS (THIS PAGE)	22. Price
[ ] Order From Sup. of Doc., U.S. Government Printing Office, Washington, DC 20402, SD Stock No. SN003-003-	UNCLASSIFIED	$4.50
[x] Order From National Technical Information Service (NTIS), Springfield, VA. 22161		